HHS Public Access

Author manuscript

Nat Neurosci. Author manuscript; available in PMC 2015 June 01.

Published in final edited form as:

Nat Neurosci. 2014 December ; 17(12): 1767–1775. doi:10.1038/nn.3868.

Short latency cerebellar modulation of the basal ganglia

Christopher H. Chen, **Rachel Fremont**, **Eduardo E. Arteaga-Bracho**, and **Kamran Khodakhah**

Dominick P. Purpura Department of Neuroscience, Albert Einstein College of Medicine, Bronx NY 10461, USA

Abstract

The graceful, purposeful motion of our body is an engineering feat which remains unparalleled in robotic devices using advanced artificial intelligence. Much of the information required for complex movements is generated by the cerebellum and the basal ganglia in conjunction with the cortex. Cerebellum and basal ganglia have been thought to communicate with each other only through slow multi-synaptic cortical loops, begging the question as to how they coordinate their outputs in real time. Here we show in mice that the cerebellum rapidly modulates the activity of the striatum via a disynaptic pathway. Under physiological conditions this short latency pathway is capable of facilitating optimal motor control by allowing the basal ganglia to incorporate time-sensitive cerebellar information and by guiding the sign of cortico-striatal plasticity. Conversely, under pathological condition this pathway relays aberrant cerebellar activity to the basal ganglia to cause dystonia.

Introduction

Basal ganglia and cerebellum are crucial for purposeful voluntary movement and perform related but distinct and complementary functions[1,2]. Their dysfunction leads to diverse motor disorders ranging from Parkinson's and Huntington's disease to loss of balance and ataxia[3,4]. Both structures are part of parallel multi-synaptic motor control loops that receive input from and send information back to the cortex[5]. To optimally control movements which require exquisite timing precision it is beneficial for these functionally related structures to communicate and coordinate their outputs in real time. Anatomical tracing studies in rodents and primates have revealed a direct disynaptic projection from the cerebellar nuclei to the basal ganglia *via* the intralaminar thalamic nuclei[6,7]. This disynaptic pathway can, in principle, provide a short latency conduit for fast communication between the cerebellum and basal ganglia thus enabling them to quickly coordinate their outputs. Yet

Please address correspondence to: Kamran Khodakhah, Dominick P. Purpura Dept. of Neuroscience, Albert Einstein College of Medicine, 1410 Pelham Pkwy South, KC 506, Bronx, NY 10461, k.khodakhah@einstein.yu.edu, Tel. (718) 430-3794.

Author Contributions:

The studies were initiated by K.K. and C.C., who designed the bulk of the experiments. C.C. performed all the experiments, except those in Figure 8. R.F. designed and performed the experiments in Figure 8. E.E.A. and C.C. designed and performed the experiments in Figures 6 and 7. All authors contributed to writing the manuscript.

A supplementary methods checklist is available.

electrophysiological studies in anaesthetized cats have only revealed slow and long latency (50–350 ms) responses in the basal ganglia following strong, repeated electrical stimulation of the cerebellum[8]. To date there is no functional evidence for the presence of rapid communication between the cerebellum and the basal ganglia. Thus whether cerebellum and basal ganglia can communicate rapidly, and indeed the utility of the disynaptic pathway as a short latency conduit between the two structures remains to be established.

Here we show, in freely moving mice, that in about half the neurons examined cerebellar stimulation effectively alters the activity of striatal neurons. Cerebellar modulation of striatal neurons had a short latency of ~10 ms, and was mediated *via* the disynaptic cerebello-thalamo-striatal pathway. We explored whether this pathway is capable of altering corticostriatal plasticity. We found that high frequency stimulation of the cortex alone predominantly depresses corticostriatal responses. However, concurrent activation of the cerebellum during high frequency stimulation of the cortex altered the direction of the plasticity resulting in the long term potentiation of corticostriatal responses. We also found that under pathological conditions the disynaptic pathway allowed for propagation of aberrant cerebellar activity to the basal ganglia. Thus we show that in an animal model of cerebellar-induced dystonia, as a consequence of aberrant cerebellar output, the activity of striatal neurons is driven to high frequency burst firing. Acutely severing the link between the cerebellum and basal ganglia by silencing the appropriate thalamic nuclei resulted in rapid alleviation of the dystonic symptoms. Our data provide good evidence in support of short latency communication between the cerebellum and the basal ganglia, and suggest that the pathway plays a crucial role in motor function and dysfunction.

Results

Short-latency Cerebellar Modulation of the Basal Ganglia

To examine whether a short latency connection between the cerebellum and the basal ganglia exists we monitored the single unit activity of neurons in the basal ganglia in awake freely moving mice while electrically or optogenetically activating the contralateral cerebellar dentate nucleus (Fig. 1–2). Recordings were obtained from the dorsolateral striatum, the input nucleus of the basal ganglia, which on the basis of anatomical tracings is the primary target of the disynaptic cerebellar projections from the dentate nuclei[9,10]. Relatively weak electrical or optogenetic stimulation of the cerebellum (mean stimulation threshold: electrical = 45±2 μA, optogenetic = 2.3±0.5 mW; Supplementary Fig. 1–2) rapidly altered the activity of striatal neurons in about half the cells examined (electrical: 78/154 neurons, 14/14 mice; optogenetic 17/33 neurons, 4/4 mice), by increasing their firing rate, decreasing it, or a combination thereof (Figs. 1–2). In all cases the extent to which the firing rate increased or decreased was correlated with the strength of cerebellar stimulation (Figure 1b–c); on average increasing the stimulation intensity by ≈20 μA more than tripled the strength of excitatory responses (Supplementary Fig. 2).

The striatum contains at least four major cell types: medium spiny neurons (MSN), fast spiking GABAergic interneurons (FSI), persistent low threshold interneurons, and also cholinergic interneurons[11,12]. It is suggested that a neuron's average firing rate and spike waveform *in vivo* can be used to identify it as either a MSN or FSI[13] : MSNs typically have

low firing rates and broad waveforms whereas FSIs on average fire at higher rates and have briefer waveforms. Cholinergic interneurons are thought to have features that are somewhat in between the two[14]. On the basis of the distribution of the spike waveform and firing rate, the responsive cells were not restricted to FSIs or MSNs and were found distributed throughout the data set (Figure 3f).

To examine how fast striatal neurons respond to cerebellar stimulation we measured response latencies in cells which were excited by cerebellar stimulation. Responses occurred rapidly after cerebellar stimulation with latencies ranging from 3–28 ms, with excitatory responses having a mean latency of 10.3±5.8 ms and a median latency of 9.0 ms (n=73; Fig. 3g). Cells recorded simultaneously on the same electrode or adjacent electrodes could have different response latencies with no correlation between presumed cell type (tentatively assigned on the basis of their spike waveforms and baseline firing rate) and response latency.

Cerebellar Inputs to the Basal Ganglia are Mediated by the Intralaminar Nuclei of the Thalamus

The short latency of cerebellar-induced striatal responses is compatible with them being mediated by the direct cerebello-basal ganglia disynaptic pathway routed through the intralaminar thalamic nuclei[9,10]. We employed two parallel approaches to test this possibility. With the first approach we optogenetically activated the cerebellar projection axons in the intralaminar nuclei (Fig. 3a–e) and examined the resulting responses in the activity of striatal neurons (Fig. 3d). Selective activation of cerebellar axons within the intralaminar thalamic nuclei was as effective as direct stimulation of the dentate nuclei in altering the activity of striatal neurons and produced comparable response types and latencies in the majority of the cells examined (14/20 cells examined, N=3; Figs. 3d–e). With the second approach we examined the consequences of inactivating the intralaminar thalamic nuclei (contralateral to the stimulation site) on cerebellar-induced striatal responses. Localized inactivation of thalamic nuclei by acute injection of QX314 or tetrodotoxin, blockers of voltage-gated sodium channels which prevent action potential generation and propagation, reversibly abolished cerebellar-induced responses in striatal neurons (7/8 attempts, 24/27 cells, N=4; Figs. 4a, Supplementary Fig. 3). These data support the hypothesis that thalamic neurons are required to convey cerebellar information to the basal ganglia. However, it is also possible that the sodium channel blockers also blocked action potential propagation in axons of passage that happen to course close to the injection site. To address this possibility we optogenetically silenced intralaminar thalamic neurons and found this also effective in blocking striatal responses to optogenetic cerebellar stimulation (n=10, N=2; Fig. 4b). This data demonstrate that neurons within the thalamic intralaminar nuclei are required for cerebellar-induced striatal responses.

It is well-established that activities of both thalamic and striatal neurons are sensitive to anesthesia[15–17], and we wondered whether this could provide an explanation as to why the short latency responses were not seen in earlier experiments carried out on anesthetized preparations[16]. Corroborating this hypothesis, we found that cerebellar-induced striatal

responses were critically dependent on the state of the animals and reversibly abated when the mice were anaesthetized (n=34, N=4; Supplementary Fig. 4).

It remains plausible, although perhaps somewhat unlikely, that the cerebellar-induced striatal responses were mediated by a thalamo-cortical pathway. In this case one could imagine that the cortex was excited by the thalamus as it relayed cerebellar information[18,19]. This increased cerebellar-induced cortical activity could then subsequently activate striatal neurons. To examine this possibility we inactivated the cortex by acutely injecting TTX or QX314 through a cannula positioned in the motor cortex. Cortical inputs provide a prominent input to the basal ganglia[20] and as expected inactivation of the cortex significantly (≈50%) reduced the spontaneous firing rate of the striatal neurons (Fig. 4c). Nonetheless after cortical inactivation cerebellar stimulations remained effective in producing short latency responses in all striatal neurons examined (n=5 cells, N=2; Fig. 4c). In three additional animals the motor cortices were surgically removed bilaterally (Supplementary Fig. 5), and the response of neurons in the dorsolateral striatum to optogenetic stimulation of the cerebellum was examined three weeks later. Even with motor cortices removed striatal neurons responded to cerebellar stimulation with the excitatory responses having an average latency of 8.4±1.2 ms (Fig. 4d; n=5 single unit and 24 multi-unit recordings; N=3). Collectively these data suggest that the short latency responses seen in dorsolateral striatum with cerebellar stimulations are most likely mediated by a direct disynaptic pathway independently of the cortex.

Striatal Activity Follows Trains of Cerebellar Stimulations

Neurons in the cerebellar output nuclei fire spontaneously at high rates and modulate their activity within a large range[3]. To determine how robustly the disynaptic pathway conveys cerebellar information when repeatedly activated, we examined the response of striatal neurons to trains of cerebellar stimulations. In all cells examined (n=32; N=5) the disynaptic pathway remained effective in producing responses in striatal neurons with trains of cerebellar stimulations as high as 50 Hz (Fig. 5).

Cerebellar Modulation of Corticostriatal Plasticity

In addition to allowing real time communication between cerebellum and basal ganglia the short latency conduit might also play a role in motor learning. It is well known that both cerebellum and the basal ganglia are required for motor learning[2] and the disynaptic cerebello-basal ganglia pathway may provide a mechanism by which the basal ganglia combine cerebellar information to optimize motor learning. In this context the reduced performance of rodents when the disynaptic connection between the two structures is severed may be, at least partially, due to suboptimal learning. This hypothesis would also account for the fact that many motor learning paradigms seem to critically require both the cerebellum and the basal ganglia[2]. Because the fidelity of synaptic communication between the motor cortex and the basal ganglia is thought to play a prominent role in motor learning[21,22] we considered the possibility that the properties and extent of cortico-striatal plasticity might be dependent, to some degree, on cerebellar input. It is known that although selective high frequency stimulation of the cortico-striatal pathway typically results in its long term depression (LTD)[23–26], the pathway can also undergo long term potentiation

(LTP)[26–28], for example if the target striatal neuron is concurrently depolarized[28]. We thus explored whether cerebellar activity could substitute for depolarization of the target striatal neuron to regulate the direction of cortico-striatal plasticity. We found, in awake freely moving mice, that following high frequency electrical stimulation of the cortico-striatal pathway in the majority of the cells activation of the cortex yielded smaller responses (Fig. 6a; 22/27 cells, N=7). Similar to that seen with striatal synaptic LTD *in vitro*[25], this weakening of the cortico-striatal response required CB1 receptors and was sensitive to intraperitoneal injection of the CB1 receptor antagonist AM-251[29] (Fig. 6b–c; n=23, N=3). We then examined whether co-activation of the cerebellum altered the extent or direction of the cortico-striatal plasticity seen following high frequency stimulation of the cortex. We found that in cells which were responsive to both cortical and cerebellar stimulation, when the same high frequency cortico-striatal stimulation was combined with concurrent 50 Hz optogenetic activation of the cerebellum (Fig. 7a) the cortico-striatal pathway was always potentiated (Fig. 7b; n=8, N=3). The potentiation of the cortico-striatal response induced by concurrent activation of the cerebellum and the cortex was long lasting (Figure 7c), and in all cases could be subsequently reversed if the cortico-striatal pathway was stimulated in the absence of cerebellar stimulation (Fig. 7d; n=5, N=3). For cerebellar stimulation to switch the sign of cortico-striatal plasticity from LTD to LTP it was necessary that the target neuron was directly excited by cerebellar stimulation. Thus even when two adjoining cells were recorded on the same electrode with one cell responsive to cerebellar stimulation and the other nonresponsive, following high frequency stimulation only the cell that was directly excited by cerebellar stimulation potentiated, whereas the other was depressed (Fig. 7e). Although the nature of our experiments prevent us from unambiguously attributing the LTP and LTD seen here *in vivo* to the synaptic plasticity characterized *in vitro*, our data nonetheless collectively support the premise that the short latency disynaptic cerebello-basal ganglia pathway allows for cerebellar modulation of the cortico-striatal plasticity.

Dynamic Cerebellar-Basal Ganglia Interactions in a Mouse Model of Rapid-Onset Dystonia Parkinsonism

The disynaptic cerebello-basal ganglia pathway has also been suggested to play a prominent, yet adverse, role under pathological conditions. For example, in an animal model of rapid onset dystonia-Parkinsonism (RDP) which is caused by loss of function mutations in the sodium pump[30] the disynaptic pathway has been speculated to be the conduit through which aberrant cerebellar activity alters the basal ganglia to cause dystonia since severing the communication by lesioning CL prevents cerebellar induction of dystonia[31]. Given the strong ability of the cerebellum in modulating basal ganglia activity described here, we wondered whether cerebellar-induced dystonia is the consequence of rapid and continuous dynamic interactions between the two structures. To directly test this hypothesis we used a previously established mouse model of RDP[31] to examine the activity of striatal neurons when dystonia was induced by selective partial block of cerebellar sodium pumps. We found that cerebellar-induced dystonic postures, monitored visually and by field electromyogram (fEMG) recordings, were temporally correlated with abnormal neuronal activity in the dorsolateral striatum (N=7; Fig. 8a). During these dystonic postures the activity of striatal neurons was transformed to high frequency burst firing (Fig. 5b–e; n = 139 cells under control and 42 cells under dystonic conditions, N=12), mimicking the bursting activity seen

in the basal ganglia of dystonic patients[32]. Moreover, consistent with the premise that the striatal neurons were driven by a common aberrant synaptic drive, during the cerebellar-induced dystonic postures there was a significant increase in cross correlation of the activity of neighboring neurons (Fig. 8f–g) with no obvious association between the striatal neurons' spike waveform characteristics and the severity of dystonia-induced burst firing. Lastly, we found that severing the link between the cerebellum and the basal ganglia by either electrically lesioning or optogenetically silencing the intralaminar thalamic neurons bilaterally by primarily targeting centrolateral (CL) nucleus of the thalamus (one of the intralaminar nuclei in rodents that hosts the bulk of the disynaptic connections[10]) alleviated cerebellar-induced dystonia (Fig. 8h–i; Supplementary video; N=6 mice for CL lesions, 3 mice and 5 trials for optogenetic inactivation of CL). In the case of optogenetic silencing of the intralaminar thalamic neurons dystonia abated within minutes if not seconds of laser activation and returned soon after termination of the light pulse.

Discussion

The cerebellum and basal ganglia are intricately related to generating well-formed movements. However, there has been little functional evidence to suggest that they can directly exchange information at timescales relevant for fast movements that they sustain. Here we show that there is a prominent short-latency pathway from the cerebellum to the basal ganglia. Under physiological conditions this pathway allows for rapid communication between the cerebellum and the basal ganglia, and permits cerebellar modulation of corticostriatal plasticity. Under pathological conditions the pathway allows for the transfer of aberrant cerebellar activity to the basal ganglia causing movement disorders such as dyskinesia and dystonia.

Potential Functional Implications of the Cerebellar Inputs to the Basal Ganglia

Cerebellar activity correlates with movement kinematics, and is necessary for the real-time adjustment and optimization of muscle activity[3]. On the other hand, it is thought that the basal ganglia are primarily concerned with the selection of optimal motor commands[1,2,33,34]. Yet, in the process of selecting the optimal motor command it seems beneficial for the basal ganglia to have the most updated information about muscle kinematics. Thus cerebellar inputs to the basal ganglia might be of value for correct action selection. Accordingly, the short latency communication delineated here might simply be in place to enable the two structures to synchronize and coordinate their activities during movements that require a high degree of timing precision.

The cerebellum is also thought to act as a predictive computational device[35,36] and the disynaptic connection may constitute a rapid pathway for communicating cerebellar predictions to the basal ganglia. In both cases the need for a short latency communication between the cerebellum and the basal ganglia is greatest when the cerebellum is expected to make a significant contribution to motor coordination, for example when movements are fast and complex. In support of this hypothesis severing the disynaptic communication by selective bilateral electrical lesion of the CL has been shown to reduce by half the

performance of rats on a cerebellar intensive rotarod task without affecting performance on stationary apparatus[37]

Cerebellar Input to Different Striatal Neurons Classes

There are numerous classes of neurons in the striatum and these are thought to play distinct roles in information processing[12,38]. Based on examination of the extracellular waveform and firing rates of the neurons from which we recorded we did not find any evidence that there are discernable predictors of which cell types will or will not receive cerebellar input. However, these parameters only allow one to unambiguously distinguish between fast-spiking interneurons and medium spiny neurons. Thus our data do not preclude the possibility that the cerebellum might have preferential input to subgroups within those populations. Anatomical tracings suggest that the disynaptic projection innervates the "indirect pathway" of the basal ganglia[9]. This would suggest that the cerebellum at least communicates with D2-receptor expressing MSNs. Whether it also has inputs to D1-receptor expressing MSNs, or specific subtypes of interneurons needs to be determined.

Corticostriatal Plasticity

We found that high frequency stimulation of the cortex depressed corticostriatal responses and, consistent with findings made *in vitro*[25], that the plasticity seen was sensitive to block by the endocannabinoid antagonist AM-251. In a small fraction of cells, however, the same high frequency stimulation potentiated the corticostriatal responses. The LTP seen in these cells may be a consequence of push/pull interactions between long term depression and potentiation mechanisms. Alternatively, given the *in vivo* nature of our preparation (behaviorally active freely moving animals), it may represent the impact of neuromodulators on the circuit[26] during specific behaviors.

We further demonstrate that simultaneous cortical and cerebellar high frequency stimulations induces long-term potentiation. The precise mechanisms of long-term potentiation in corticostriatal inputs is unclear, although it is thought to involve postsynaptic NMDA receptors[26–28]. It is plausible that cerebellar input depolarizes striatal cells, and that this depolarization is sufficient to prime NMDA receptors for coincident input from the cortex. Alternatively, dopamine may play a role *via* intrastriatal release through cerebellar activation of interneurons[39], or cerebellar activation of the substantia nigra[40,41].

Interestingly, our report is not the first hint for cerebellar involvement in corticostriatal plasticity. It has been previously shown that corticostriatal LTD is not present in animals with contralateral cerebellar hemispherectomies[42]. Given our findings, it may be the case that cerebellar-striatal potentiation balances corticostriatal depression; without cerebellar input corticostriatal long-term depression saturates to a level where further depression does not occur.

Cerebello-thalamo-striatal circuitry and dystonia

We find that in an animal model of a cerebellar-induced dystonia the neurons of the dorsolateral striatum exhibit abnormal high-frequency burst firing. Similar high frequency burst firing has been noted in the basal ganglia of dystonic patients[43,44]. Based on these

observations it is possible that bursting activity in the basal ganglia may be the common substrate that causes dystonia in different dystonias – independent of whether the burst firing is caused by intrinsic defects in the basal ganglia, or whether it is driven by aberrant input from other structures. On the basis of the data presented it is also clear that acutely silencing the connection between the cerebellum and basal ganglia alleviates dystonia. Thus, in cases where the cerebellum is known to cause dystonia, surgically disrupting (by lesioning or DBS) the human thalamic nuclei that accommodate the disynaptic pathway may be a viable therapeutic approach. In fact, interventions involving the thalamus have been shown to produce immediate alleviation of dystonic symptoms in a number of patients[45,46].

It is interesting to note that in a rodent model of the genetic dystonia DYT1 corticostriatal LTD is saturated[47]. Since we demonstrate here that cerebello-striatal connections normally mediate LTP, it is possible that in DTY1 mice a change in chronic cerebellar activity disrupts the normal LTP mediated by this pathway. This could leave corticostriatal LTD unopposed and result in its saturation. The relationship of such changes in basal ganglia plasticity to dystonia remains to be established, particularly since the genetic mouse models of DYT1 do not manifest dystonia even though they show saturated corticostriatal LTD.

Conclusions

The robust and rapid cerebellar modulation of basal ganglia described here provides a key insight as to how these two structures communicate in health and disease. Future scrutiny will no doubt unravel the nature of the information that is conveyed from the cerebellum to the basal ganglia, and any topographic organization of this pathway. Given that both the cerebellum and the basal ganglia have also been implicated in non-motor tasks, it would be interesting to examine whether cerebellar modulation of basal ganglia activity also extends to its cognitive functions. It is interesting to note that a reverse cortex-independent pathway from the basal ganglia to the cerebellum has also been described anatomically[48]. It would be important to determine the functional efficacy of this connection, and to explore whether it provides a conduit for short latency transfer of information in the opposite direction to that delineated here, thereby providing for bidirectional real time communication between these two motor structures.

Methods

Experiments were conducted on 10–40 week-old C57/BL6 mice in accordance with guidelines set by Albert Einstein College of Medicine. Mice were housed on a 12:12 reversed light/dark cycle. Mice were allowed to recover for at least four days after surgery and housed individually. When brain regions were stimulated or inhibited optogenetically, experiments began > 2.5 weeks after surgery to allow for optimal opsin expression.

Single unit microwire recordings and data analysis

All experiments were performed during the mouse's dark cycle. Single unit recordings were made unilaterally from dorsolateral striatum using custom-made eight wire drivable microarrays[49]. The microarray consisted of 100 μm Teflon insulated tungsten wires (50 μm core, AM Systems) assembled into two by four arrays (0.4 mm by 0.8 mm) and fixed into a

custom-made screw drive (FineLine Prototyping). Arrays were implanted into the dorsolateral striatum (ML 2.5 mm; AP 0.55 mm; 1.2mm from the surface of the brain).

Microwire arrays were advanced 75 or 150 μm per day as needed with a maximum total advancement of 1.5 mm. This range ensured that recordings were limited to the dorsal aspect of the striatum. The correct positioning of the recording and stimulation wires were ascertained histologically postmortem. To do so, at the end of the recording schedule a 60 μA 30 s long current was used to lesion the brain. Animals were then killed with a lethal dose of halothane and transcardially perfused sequentially with PBS and 4% paraformaldehyde. Brains were extracted and post-fixed in 4% paraformaldehyde for at least 24h and then cryoprotected in 30% sucrose for 1–3 days. Brains were sectioned at 50 μm and Nissl stained (Supplementary material 1).

Single unit signals were amplified 5000× using a headstage (TuckerDavis Technologies) and a homemade amplifier (150 Hz–10 kHz, RC bandpass filter) and digitized at 20 kHz with a National Instruments card (PCI-MIO-16XE) using custom-written software in Labview. Signals were wavelet filtered[50] in Matlab (Mathworks) and sorted offline using principle component analysis (Offline Sorter, Plexon). Units with amplitudes <4× (signal σ) were excluded from the analysis. Waveforms were quantified in Matlab with valley and peak referring to the negative and the positive deflections of the waveforms corresponding with the rising phase and the downstroke of the cell's action potential.

Post stimulus firing rate histograms (PSTHs) were generated in Matlab. Bins were set to 2 ms. Response latencies for cells with excitation were determined by finding the first bin which was at least 3σ greater than the baseline firing rate.

Change in the number of spikes fired and response types (excitation, inhibition, or both) were calculated from regions of interest set in the average PSTH. An initial set of seed boundaries were set by the experimenter and bounds were then narrowed by an automated script written in Matlab using a defined set of parameters as follows: 1) an excitatory response started when the instantaneous firing rate was more than 3σ above the baseline firing rate, and terminated when it declined below this threshold, 2) the start of inhibition was defined as a decrease in the firing rate 1σ below the baseline firing rate for at least 10 ms, and the end of inhibition was defined as when the firing rate returned to baseline.

Electrical and optogenetic cerebellar stimulations

To stimulate the cerebellar dentate nucleus, all mice were implanted with a stimulating electrode or a fiber optic implant contralateral to the basal ganglia recording side. At least 200 trials per intensity were obtained with both electrical and optogenetic stimulations.

For electrical stimulation, a twisted bipolar electrode (PlasticsOne, ≈130 kΩ impedance) was implanted using the coordinates: ML –2.3 mm; AP –6.00 mm; 2.4 mm from the surface of the brain. Electrical stimuli were delivered as 200 μs constant current or voltage pulses ranging from 1 to 10 V or 10 to 100 μA (in all cases the strength of electrical stimulations are reported in terms of current taking into consideration the impedance of the stimulation electrodes).

To optogenetically excite cells we used an AVV vector to express the light-sensitive cation channel, channelrhodopsin, in the target cells and then as needed activated the channels be exposing them to light of the appropriate wavelength. To optically stimulate the dentate nucleus, 1 μl of AAV2-Syn-ChR2(H134R)-YFP (University of North Carolina Vector Core) or 0.7 μl of AAV2/1-Syn-ChR2(H134R)-YFP (University of Pennsylvania Vector Core) was injected into the same coordinates at a rate of 0.1 μl/min. An optical fiber (200 μm diameter, 0.48 NA, Thorlabs) was subsequently implanted in the injection site to deliver light during the experiment. The exact location where ChR2 was expressed, and the position of the fiber optic was ascertained histologically. To visualize expression of ChR2 and ArchT tissue was stained with rabbit anti-GFP antibody (Molecular Probes by Life Technologies, Cat. No. A11122) conjugated with Alexa Fluor 488 and counter stained with Hoechst 33342 (Molecular Probes, Eugene, Oregon). Postmortem anti-GFP staining and fluorescence microscopy confirmed the expression and appropriate selective targeting of ChR2 to the dentate nucleus (see Supplementary data). Optical stimuli were delivered as 10 ms pulses using a 450 nm or 473 nm laser (OEM Laser Systems). Reported light powers correspond to the light intensity at the tip of the fiber optic exposed to tissue. Stimuli ranged from 0.5 mW to 5 mW.

Three sets of experiments were done to ascertain that optogenetic cerebellar stimulations activated cerebellar nuclei neurons by activating ChR2. First, ChR2 takes several weeks to optimally get expressed in neurons, and in all animals examined stimulations at maximum intensity did not produce a response for at least 10 days post-surgery, suggesting that it was ChR2 expression, rather than non-specific actions of light in the cerebellum that mediated the responses. Second, strong optical stimulations (>10 mW) using a 640 nm that does not activate ChR2 never produced a response whereas much lower intensity stimulations using the appropriate 450 or 473 nm lasers were very effective. Third, single-unit recordings were made in a head-restrained, awake mouse expressing ChR2 in the dentate nucleus of the cerebellum using a custom-made optrode. Brief (10 ms) pulses of light reliably increased the firing rate of the neuron recorded (Supplementary Data 1).

Inactivation of the thalamus

To chemically inactivate the thalamus with the sodium channel blockers TTX or QX314, we used previously published set of injection parameters that ensure selective, localized perfusion of brain structures[31]. Briefly, a subset of mice were implanted with a 26 gauge guide cannula (Small Parts) targeting the centrolateral nucleus of the thalamus (AP –1.58 mm; ML –0.8 mm; 3 mm from the brain's surface; ipsilateral to the recording site). An acute injector (Plastics One) connected to an automated pump was placed in the guide cannula and 1 μl of 100 mM QX-314 or 50 mM tetrodotoxin (Tocris) was infused through the injector at a rate of 0.2 μl/min. Typically, attenuation of cerebellar responses began 20 minutes after infusion onset, remained effective for at least 30 minutes and washed out about an hour later.

In a few mice the intralaminar nuclei were silenced optogenetically by expressing the light sensitive proton transporter archaerhodopsin in the target cells. To do so, 1 μl AAV2/2-CAG-ArchT-GFP (University of North Carolina Vector Core) was injected in the same

coordinates delineated above at a rate of 0.1 μl/min. An optical fiber (200 μm diameter, 0.48 NA, Thorlabs) was then implanted targeting CL. Optical inhibition of the thalamus was achieved using a 640 nm laser (OEM Laser Systems) with a power of 5–10 mW. The laser was turned on 500 ms before cerebellar stimulation and turned off 500 ms after. Postmortem anti-GFP staining and fluorescence microscopy was used to confirm the expression and appropriate targeting of ArchT to the intralaminar thalamic nuclei in addition to the position of the fiber optic within the structure.

Silencing of the motor cortex

To chemically inactivate the motor cortex, two stainless steel 26 gauge cannulas (Small Parts) were implanted in the cortex (ML 1.5 mm; AP 1.55/–0.55 mm; 0.5 mm from brain surface). 2–3 V (set at the threshold for eliciting overt movements) 200 μs pulses were applied to the cannulas. Once a striatal response was observed, 3 μl of 50 mM TTX or 100 mM QX-314 was infused at 0.2 μl/min through the cannula which had produced the largest response in the target striatal neuron. Typically within 20–30 minutes after onset of infusion of the blocker the firing rate of the target striatal neuron decreased.

To surgically remove the motor cortex, a large section of the skull was removed and the cortex was aspirated. Four points marking the corners of a rectangle were used to identify the area for aspiration. They were: ML ±2 mm, AP 2.5 mm and ML ± 1 mm, AP –1 mm. During aspiration, the white matter tracts of the corpus callosum were used to reference the depth of ablation and used as a lower limit for the aspirator (≈ 1 mm). The cavity was then filled with gelfoam for recovery. Recordings were made from these mice three weeks after removal of the cortex.

Stimulation of the motor cortex, and cortico-striatal plasticity

To stimulate the motor cortex, a metal tube (14 gauge, Small Parts) was integrated into the bottom edge of the microdrive containing the microwire array. This metal tube was implanted 0.5 mm into the motor cortex and used for stimulation. To test striatal responses to cortical stimulation, 200 μs voltage pulses ranging from 1 to 4 V were used. These intensities corresponded to 6 μA–22 μA respectively. To confirm that electrodes were implanted in the motor cortex and to determine the maximum stimulus intensity, stimulus intensity was gradually increased until they elicited movements. The highest intensity that did not illicit movements was used to probe cortico-striatal inputs and was subsequently also used for plasticity induction.

The high frequency stimulus (HFS) protocol used to induce cortico-striatal plasticity consisted of a train of 100 Hz pulses for 1 second, repeated 4 times with 10 second intervals between the trains. This was delivered to the motor cortex as described above. Only striatal cells that showed an excitatory response to cortical stimulation or excitation followed by inhibition were considered for analysis, although only the impact of the plasticity paradigm on the excitatory component was quantified.

To test whether the weakening of the corticostriatal response following high frequency stimulation was dependent on endocannabinoids, we administered AM-251 at least 30 minutes before starting experiments. AM-251 was dissolved in 20% DMSO and 80%

distilled water and injected at 5 mg/kg. Experiments continued as discussed in the previous paragraph. To potentiate cortico-striatal responses, in addition to the motor cortex the cerebellum was also stimulated with a high frequency train although cerebellar stimulations were performed optogenetically. Cortical stimulation trains were delivered as described above. Cerebellar HFS consisted of a train of 50 Hz light pulses for 1 second, repeated 4 times with an interval of 10 seconds. Thus, both the cerebellar and cortical trains occurred concurrently. Two criteria had to be satisfied prior to start of such a plasticity protocol. First, the striatal neuron's response to cerebellar stimulation had to be excitatory. And second, the striatal neuron needed to show a sustained increase in its firing rate when the cerebellum was excited with 5 pulses at 50 Hz (Figure 7).

Field EMG and striatal recordings in mice with cerebellar-induced dystonia

To examine the role of cerebello-basal ganglia interactions in cerebellar-induced dystonia, we used a previously established mouse model of Rapid Onset Dystonia Parkinsonism which is caused by loss of function mutations in the sodium pump. In this mouse model acute or chronic perfusion of ouabain, a selective blocker of sodium pumps, into the cerebellum is sufficient to cause dystonia[31]. In a single surgery, a cannula was implanted into the cerebellum and a microwire array was implanted into the dorsolateral striatum. Once baseline recordings were made from dorsolateral striatal neurons as described, dystonia was acutely induced by infusing ouabain (100 μM) into the cerebellum *via* the cannula at a rate of 0.3 μl/minute following previously published procedures[31]. This allowed for direct comparison of the activity of some cells before and after induction of dystonia.

To monitor the time of onset of dystonic postures, we also performed field electromyogram (fEMG) recordings[31] by inserting a wire under the skin on the back of the animal approximately half way between the neck and the tail. The position of the recording electrodes and the perfusion cannula were ascertained postmortem by histology as described earlier.

Alleviation of cerebellar-induced dystonia by electrical lesioning of CL

It is already established that bilaterally lesioning CL prevents induction of cerebellar-induced dystonia[31]. We explored whether electrical lesion of CL can alleviate previously generated cerebellar-induced dystonia. To be able to follow dystonic animals for several days after electrically lesioning CL we generated the long lasting form of dystonia by chronically perfusing ouabain into the cerebellum as previously described[31]. A single cannula was stereotaxically implanted at the cerebellar midline (AP:–6.90 mm from bregma and DV: 2mm) and connected to an osmotic pump (0.25 μl/h, Alzet) containing ouabain (100 μM) and 0.01% methylene blue, which allowed for post-mortem examination of the perfusion site. The pump was then placed under the skin on the back of the mice. With this procedure mice showed dystonia within 24 hours after the surgery.

To be able to lesion the CL once dystonia was induced, in the same surgery custom made electrodes were bilaterally implanted into CL (AP, –1.58 mm from Bregma; DV, 3.5 mm; ML, 0.8 mm and –0.8 mm). After onset of dystonia, lesions were made using 300 μA, 45 seconds long current pulses at each CL site. Since the disynaptic pathway passes through the

posterior 2/3 of CL in rodents, we targeted the posterior portion of this nucleus. The extent and location of lesions were determined histologically using Nissl staining as reported previously[31]. Only mice in which the specificity of CL lesions was histologically confirmed were included in the analysis. The efficacy of the CL lesions in alleviating dystonia was evaluated 24 hours after the lesion.

Alleviation of cerebellar-induced dystonia by optogenetic inactivation of the CL

The intralaminar nuclei and primarily the CL were optogenetically silenced and the impact on cerebellar-induced dystonia examined. In a single surgery, 1 μl AAV2/5-CAG-ArchT-GFP (University of North Carolina Vector Core) was injected into CL (AP, –1.58 mm from Bregma; DV, 3.5 mm; ML, 0.8 mm and –0.8 mm), fiber optics were implanted immediately above the injection site to target the CL, and an infusion cannula was implanted into the cerebellum (AP:–6.90 mm from bregma and DV: 2mm). After 2 weeks for opsin expression, dystonia was induced by infusing ouabain (100 μM) into the cerebellum *via* the cannula at a rate of 0.3 μl/minute as described earlier. Once dystonia manifested, the intralaminar nuclei were silenced by activating a 640 nm laser (OEM Laser Systems) with a power of 5–10 mW.

Dystonia Score

The presence of dystonia and its severity were quantified using a previously published scale[31]. Briefly, 0 = normal behavior; 1 = abnormal motor behavior, no dystonic postures; 2 = mild motor impairment, dystonic-like postures when disturbed; 3 = moderate impairment, frequent spontaneous dystonic postures; 4 = severe impairment, sustained dystonic postures. The assessment of dystonia was made independently by three trained observers blinded to the condition of the mice. All three observers scored the same video clips. Their scores were averaged by the authors.

Statistical analyses

We examined the variance within each group with the F test and determined whether the data exhibited a Gaussian distribution with the D'Agostino-Pearson omnibus normality test. We analyzed the data using parametric (two-samples, one/two-tailed Student's t-test or ANOVA) or non-parametric (one/two-tailed Mann-Whitney U, Kruskal-Wallis, paired or one sample Wilcoxon signed ranks) depending on whether the data displayed or did not display a Gaussian distribution, equal variance or similar sample size. We compared the observed proportion of distributions using the chi-square test for goodness of fit. To estimate ideal sample sizes, power analyses were conducted using the first few experiments to determine mean and standard deviation based on the magnitude of the anticipated effect (power 0.90 with a significance value of 0.05). Sample sizes for experiments alleviating dystonia were determined from previously published experiments. All experiments met or exceeded ideal sample sizes.

Supplementary Material

Refer to Web version on PubMed Central for supplementary material.

Acknowledgments

We thank the members of the Khodakhah laboratory for invaluable discussions and comments on the manuscript.

References

1. Doya K. What are the computations of the cerebellum, the basal ganglia and the cerebral cortex? Neural Netw. 1999; 12:961–974. [PubMed: 12662639]
2. Doya K. Complementary roles of basal ganglia and cerebellum in learning and motor control. Curr Opin Neurobiol. 2000; 10:732–739. [PubMed: 11240282]
3. Ito, M. The cerebellum and neural control. Raven Press; New York: 1984.
4. Albin RL, Young AB, Penney JB. The functional anatomy of basal ganglia disorders. Trends Neurosci. 1989; 12:366–375. [PubMed: 2479133]
5. Middleton FA, Strick PL. Basal ganglia and cerebellar loops: motor and cognitive circuits. Brain Res Brain Res Rev. 2000; 31:236–250. [PubMed: 10719151]
6. Ichinohe N, Mori F, Shoumura K. A di-synaptic projection from the lateral cerebellar nucleus to the laterodorsal part of the striatum via the central lateral nucleus of the thalamus in the rat. Brain Res. 2000; 880:191–197. [PubMed: 11033006]
7. Hoshi E, Tremblay L, Feger J, Carras PL, Strick PL. The cerebellum communicates with the basal ganglia. Nat Neurosci. 2005; 8:1491–1493. [PubMed: 16205719]
8. Ratcheson RA, Li CL. Effect of dentate stimulation on neuronal activity in the caudate nucleus. Exp Neurol. 1969; 25:268–281. [PubMed: 5345013]
9. Hoshi E, Tremblay L, Feger J, Carras PL, Strick PL. The cerebellum communicates with the basal ganglia. Nat Neurosci. 2005; 8:1491–1493. [PubMed: 16205719]
10. Ichinohe N, Mori F, Shoumura K. A di-synaptic projection from the lateral cerebellar nucleus to the laterodorsal part of the striatum via the central lateral nucleus of the thalamus in the rat. Brain Res. 2000; 880:191–197. [PubMed: 11033006]
11. Kreitzer AC. Physiology and pharmacology of striatal neurons. Annual review of neuroscience. 2009; 32:127–147.
12. Gittis AH, Nelson AB, Thwin MT, Palop JJ, Kreitzer AC. Distinct roles of GABAergic interneurons in the regulation of striatal output pathways. J Neurosci. 2010; 30:2223–2234. [PubMed: 20147549]
13. Berke JD, Okatan M, Skurski J, Eichenbaum HB. Oscillatory entrainment of striatal neurons in freely moving rats. Neuron. 2004; 43:883–896. [PubMed: 15363398]
14. Schwingenschuh P, et al. Distinguishing SWEDDs patients with asymmetric resting tremor from Parkinson's disease: a clinical and electrophysiological study. Movement disorders : official journal of the Movement Disorder Society. 2010; 25:560–569. [PubMed: 20131394]
15. Lacey CJ, Bolam JP, Magill PJ. Novel and distinct operational principles of intralaminar thalamic neurons and their striatal projections. J Neurosci. 2007; 27:4374–4384. [PubMed: 17442822]
16. Ratcheson RA, Li CL. Effect of dentate stimulation on neuronal activity in the caudate nucleus. Exp Neurol. 1969; 25:268–281. [PubMed: 5345013]
17. Llinas RR, Steriade M. Bursting of thalamic neurons and states of vigilance. J Neurophysiol. 2006; 95:3297–3308. [PubMed: 16554502]
18. Van der Werf YD, Witter MP, Groenewegen HJ. The intralaminar and midline nuclei of the thalamus. Anatomical and functional evidence for participation in processes of arousal and awareness. Brain research. Brain research reviews. 2002; 39:107–140. [PubMed: 12423763]
19. Proville RD, et al. Cerebellum involvement in cortical sensorimotor circuits for the control of voluntary movements. Nat Neurosci. 2014; 17:1233–1239. [PubMed: 25064850]
20. Stern EA, Kincaid AE, Wilson CJ. Spontaneous subthreshold membrane potential fluctuations and action potential variability of rat corticostriatal and striatal neurons in vivo. J Neurophysiol. 1997; 77:1697–1715. [PubMed: 9114230]
21. Koralek AC, Jin X, Long JD 2nd, Costa RM, Carmena JM. Corticostriatal plasticity is necessary for learning intentional neuroprosthetic skills. Nature. 2012; 483:331–335. [PubMed: 22388818]

22. Houlden H, et al. THAP1 mutations (DYT6) are an additional cause of early-onset dystonia. Neurology. 2010; 74:846–850. [PubMed: 20211909]
23. Calabresi P, Maj R, Pisani A, Mercuri NB, Bernardi G. Long-term synaptic depression in the striatum: physiological and pharmacological characterization. J Neurosci. 1992; 12:4224–4233. [PubMed: 1359031]
24. Kreitzer AC, Malenka RC. Endocannabinoid-mediated rescue of striatal LTD and motor deficits in Parkinson's disease models. Nature. 2007; 445:643–647. [PubMed: 17287809]
25. Gerdeman GL, Ronesi J, Lovinger DM. Postsynaptic endocannabinoid release is critical to long-term depression in the striatum. Nat Neurosci. 2002; 5:446–451. [PubMed: 11976704]
26. Shen W, Flajolet M, Greengard P, Surmeier DJ. Dichotomous dopaminergic control of striatal synaptic plasticity. Science. 2008; 321:848–851. [PubMed: 18687967]
27. Calabresi P, Pisani A, Mercuri NB, Bernardi G. Long-term Potentiation in the Striatum is Unmasked by Removing the Voltage-dependent Magnesium Block of NMDA Receptor Channels. Eur J Neurosci. 1992; 4:929–935. [PubMed: 12106428]
28. Charpier S, Deniau JM. In vivo activity-dependent plasticity at cortico-striatal connections: evidence for physiological long-term potentiation. Proc Natl Acad Sci U S A. 1997; 94:7036–7040. [PubMed: 9192687]
29. Hilario MR, Clouse E, Yin HH, Costa RM. Endocannabinoid signaling is critical for habit formation. Front Integr Neurosci. 2007; 1:6. [PubMed: 18958234]
30. De Carvalho AP, et al. Mutations in the Na+/K+ -ATPase alpha3 gene ATP1A3 are associated with rapid-onset dystonia parkinsonism. Neuron. 2004; 43:169–175. [PubMed: 15260953]
31. Calderon DP, Fremont R, Kraenzlin F, Khodakhah K. The neural substrates of rapid-onset Dystonia-Parkinsonism. Nat Neurosci. 2011; 14:357–365. [PubMed: 21297628]
32. Starr PA, et al. Spontaneous pallidal discharge in 15 cases of dystonia: Comparison with Parkinson's disease and normal Macaque. Movement Disorders. 2004; 19:S90–S90.
33. Redgrave P, Prescott TJ, Gurney K. The basal ganglia: a vertebrate solution to the selection problem? Neuroscience. 1999; 89:1009–1023. [PubMed: 10362291]
34. Mink JW. The basal ganglia: focused selection and inhibition of competing motor programs. Prog Neurobiol. 1996; 50:381–425. [PubMed: 9004351]
35. Medina JF. The multiple roles of Purkinje cells in sensori-motor calibration: to predict, teach and command. Current opinion in neurobiology. 2011; 21:616–622. [PubMed: 21684147]
36. Miall RC, Weir DJ, Wolpert DM, Stein JF. Is the Cerebellum a Smith Predictor. Journal of motor behavior. 1993; 25:203–216. [PubMed: 12581990]
37. Jeljeli M, Strazielle C, Caston J, Lalonde R. Effects of centrolateral or medial thalamic lesions on motor coordination and spatial orientation in rats. Neuroscience Research. 2000; 38:155–164. [PubMed: 11000442]
38. Paille V, et al. GABAergic circuits control spike-timing-dependent plasticity. J Neurosci. 2013; 33:9353–9363. [PubMed: 23719804]
39. Threlfell S, et al. Striatal dopamine release is triggered by synchronized activity in cholinergic interneurons. Neuron. 2012; 75:58–64. [PubMed: 22794260]
40. Nieoullon A, Cheramy A, Glowinski J. Release of dopamine in both caudate nuclei and both substantia nigrae in response to unilateral stimulation of cerebellar nuclei in the cat. Brain Res. 1978; 148:143–152. [PubMed: 656921]
41. Nieoullon A, Dusticier N. Changes in dopamine release in caudate nuclei and substantia nigrae after electrical stimulation of the posterior interposate nucleus of cat cerebellum. Neurosci Lett. 1980; 17:167–172. [PubMed: 7052460]
42. Rossi S, et al. Cerebellar control of cortico-striatal LTD. Restor Neurol Neurosci. 2008; 26:475–480. [PubMed: 19096135]
43. Starr PA, et al. Spontaneous pallidal neuronal activity in human dystonia: comparison with Parkinson's disease and normal macaque. Journal of neurophysiology. 2005; 93:3165–3176. [PubMed: 15703229]
44. Vitek JL, et al. Neuronal activity in the basal ganglia in patients with generalized dystonia and hemiballismus. Ann Neurol. 1999; 46:22–35. [PubMed: 10401777]

45. Cooper IS. Clinical and physiologic implications of thalamic surgery for disorders of sensory communication. 2. Intention tremor, dystonia, Wilson's disease and torticollis. J Neurol Sci. 1965; 2:520–553. [PubMed: 5878841]

46. Horisawa S, Taira T, Goto S, Ochiai T, Nakajima T. Long-term improvement of musician's dystonia after stereotactic ventro-oral thalamotomy. Annals of neurology. 2013; 74:648–654. [PubMed: 23463596]

47. Martella G, et al. Impairment of bidirectional synaptic plasticity in the striatum of a mouse model of DYT1 dystonia: role of endogenous acetylcholine. Brain. 2009; 132:2336–2349. [PubMed: 19641103]

48. Bostan AC, Dum RP, Strick PL. The basal ganglia communicate with the cerebellum. Proc Natl Acad Sci USA. 2010

49. du Hoffmann J, Kim JJ, Nicola SM. An inexpensive drivable cannulated microelectrode array for simultaneous unit recording and drug infusion in the same brain nucleus of behaving rats. J Neurophysiol. 2011; 106:1054–1064. [PubMed: 21613588]

50. Wiltschko AB, Gage GJ, Berke JD. Wavelet filtering before spike detection preserves waveform shape and enhances single-unit discrimination. Journal of neuroscience methods. 2008; 173:34–40. [PubMed: 18597853]

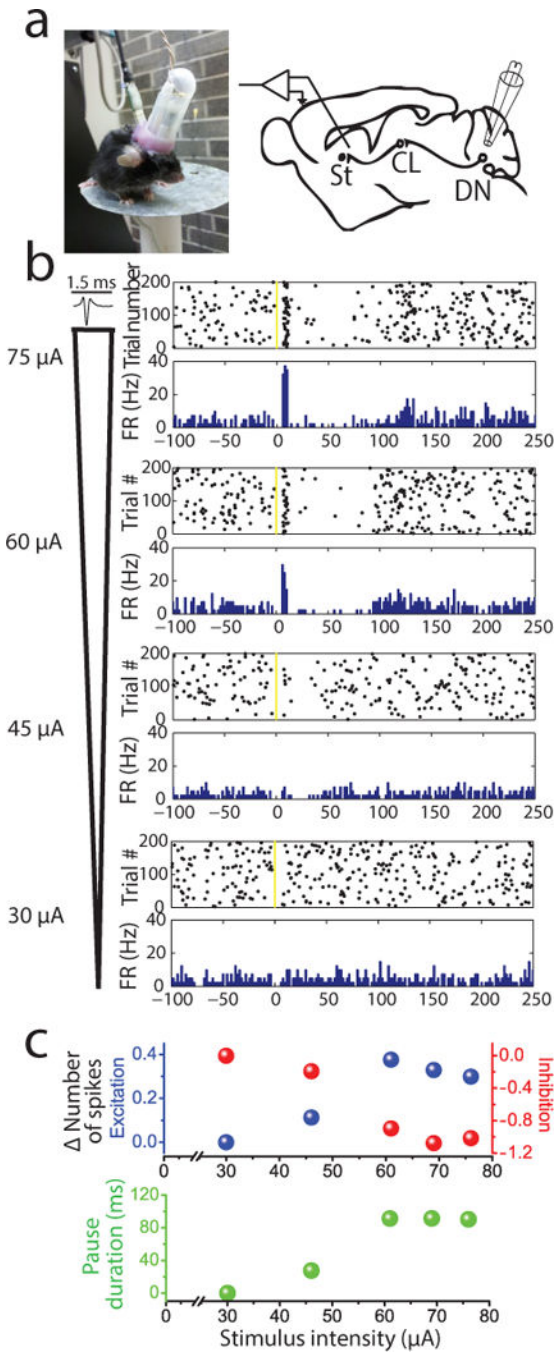

Figure 1. Striatal responses to cerebellar stimulation

(a) Single-unit activity of dorsolateral striatal neurons were monitored in awake freely moving mice while electrically stimulating the contralateral dentate cerebellar nucleus. (b) Responses of a striatal neuron to cerebellar stimulations at various intensities. Rasters obtained from 200 trials at each intensity are shown together with the corresponding post – stimulus firing rate histogram. Yellow bar denotes the timing of the stimulus, and the neuron's average waveform is displayed on the top-left.

(c) Quantification of cell shown in “b”. The change in number of spikes for the excitatory and inhibitory phases is shown in the top panel in blue and red respectively. The pause duration is shown in green in the bottom panel.

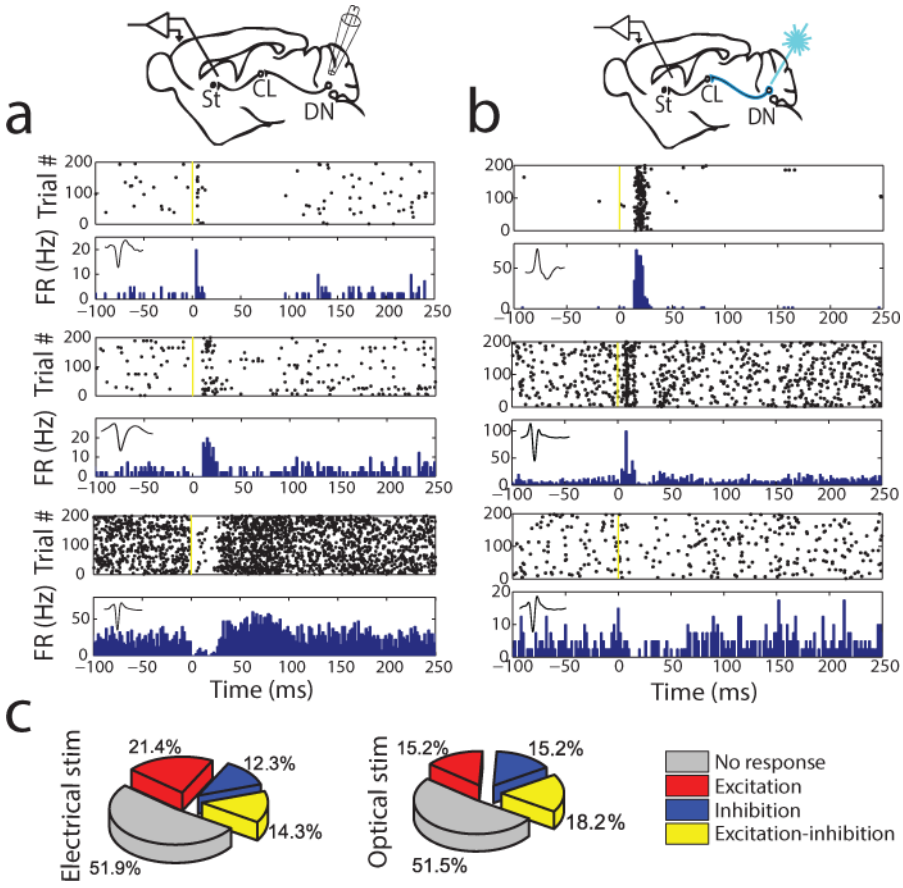

Figure 2. Diversity of striatal responses to cerebellar stimulation

Single-unit responses of dorsolateral striatal neurons in awake freely moving mice to (a) electrical, or (b) optogenetic stimulation of the centrolateral cerebellar dentate nucleus. In both cases three general types of responses are seen: excitation, excitation followed by inhibition, and inhibition. Each neuron's average waveforms is shown as an inset in each raster.

(c) Percent of cells responding to electrical stimulation (n=154, N=14) and optogenetic stimulation (n=33, N=4).

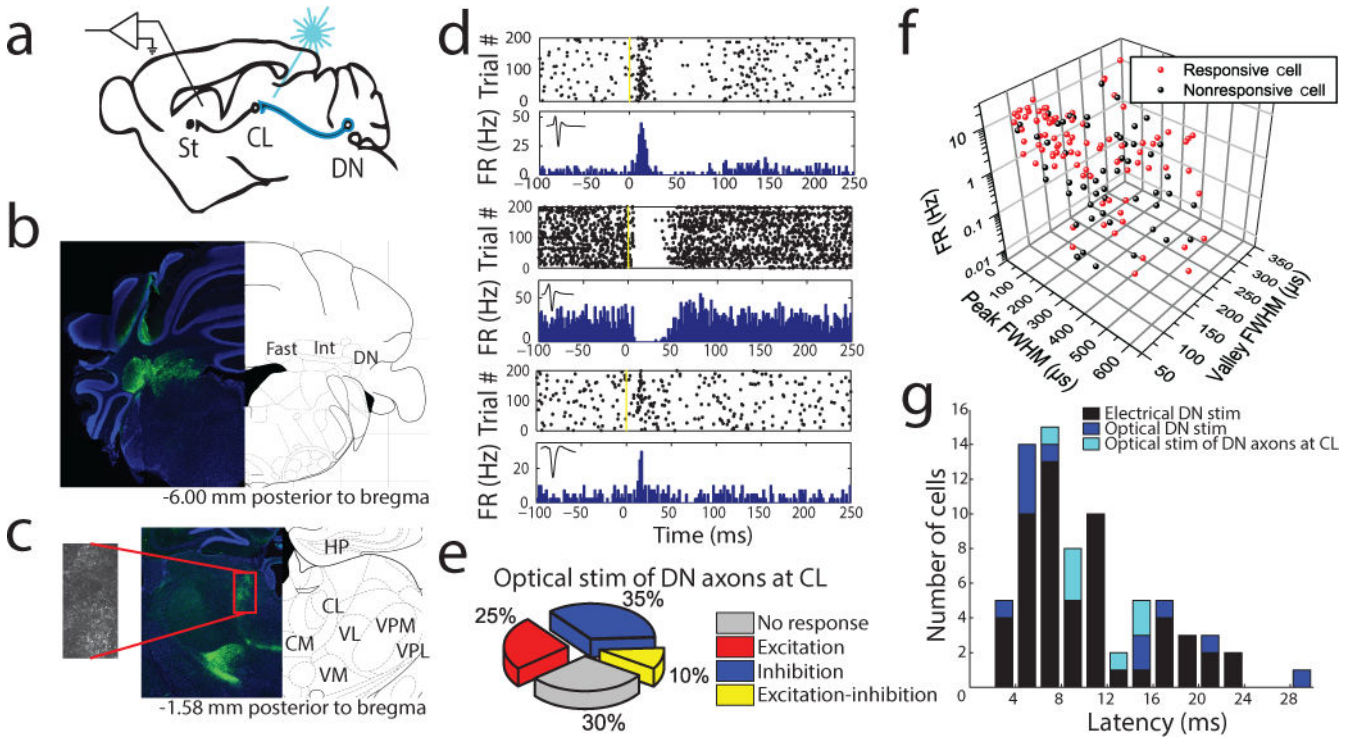

Figure 3. Striatal responses to stimulation of cerebellar axons in the centrolateral thalamus

(a) Schematic of experimental design. Microwire arrays were implanted in the dorsolateral striatum (St), ChR2 was expressed in the dentate nucleus of the cerebellum (DN), and the optical fiber was implanted in the CL ipsilateral to the microwire implant.

(b,c) Expression of ChR2 in the injection site (b) and thalamus (c). ChR2 expression is shown in green; DAPI staining in blue. Cerebellar axons expressing ChR2 are present in multiple thalamic regions. Inset magnification: 20X. Abbreviations: Fast: fastigial nucleus; Int: interposed nucleus; and DN: dentate nucleus of the cerebellum; HP: hippocampus; CL: centrolateral thalamus; CM: centromedian nucleus; VL: ventrolateral thalamus; VM: ventromedial thalamus; VPM: ventral posteromedial thalamus; VPL: ventral posterolateral thalamus.

(d) Example responses to optogenetic stimulation of cerebellar projection axons within the CL and surrounding intralaminar thalamic nuclei.

(e) Percent of cells responding with each response type to optogenetic stimulation of cerebellar axons in the CL (n=20, N=3).

(f) Firing rate and waveform characteristics of every dorsolateral striatal neuron which showed a response (red), or was unaffected (black) by electrical or optogenetic stimulation of the cerebellum.

(g) Excitatory response latencies of striatal neurons following cerebellar activation using electrical DN stimulation, optogenetic DN stimulation, or optogenetic stimulation of cerebellar axons in the thalamus.

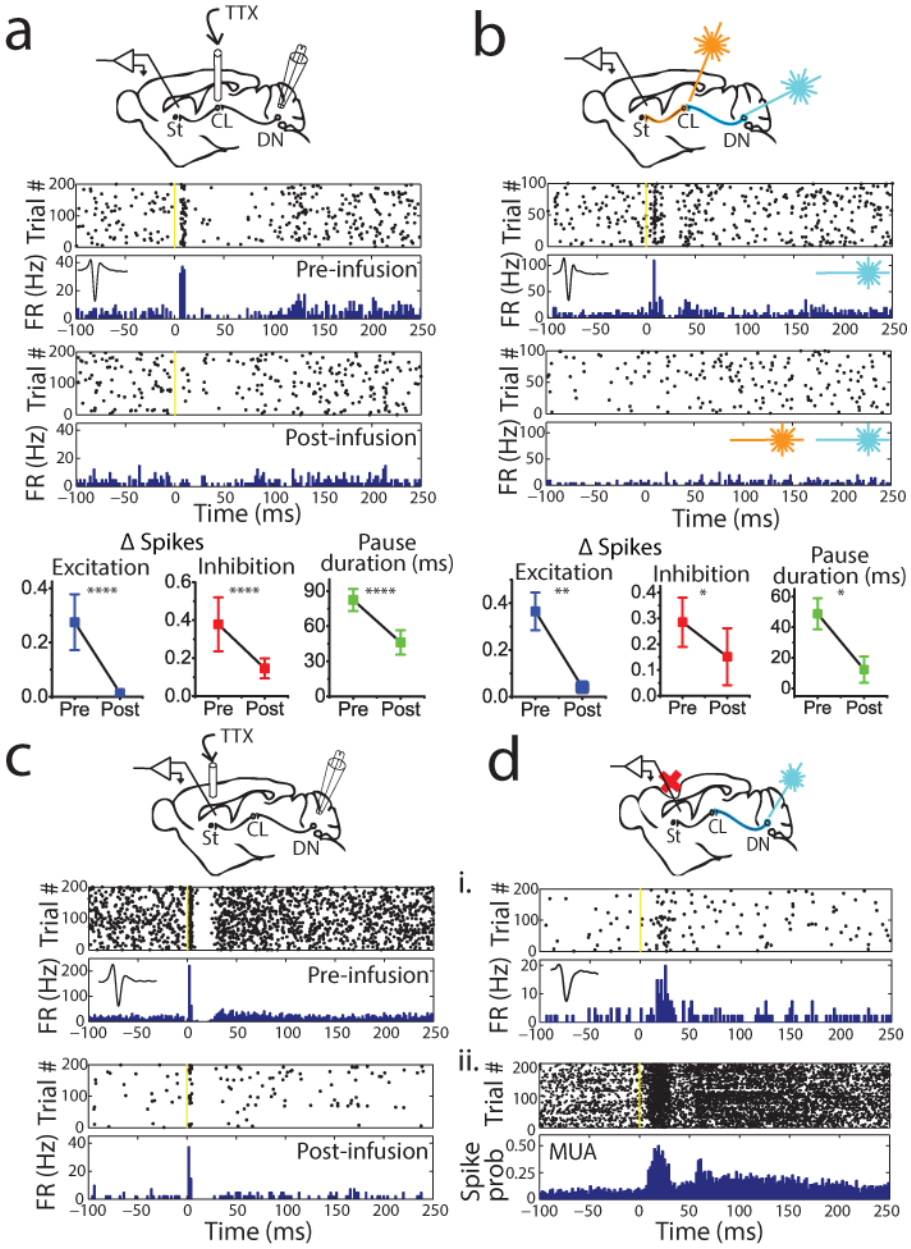

Figure 4. Cerebellar evoked striatal responses are mediated by the disynaptic pathway

(a) Inactivation of the thalamus by microinjection of QX-314 or TTX blocked cerebellar-induced responses in striatal neurons. An example cell is shown on top panels. Summary data for the change in the number of spikes during excitatory and inhibitory phases of the response and the change in pause duration are shown on the bottom. Data are displayed as mean±S.E.M. ****=p<0.0001; one tailed Wilcoxon paired signed ranks test. (n=24, N=4)

(b) Optogenetic inactivation of the intralaminar nuclei by primarily optically targeting CL blocked cerebellar-induced responses in striatal neurons. Summary data as in (a). *=p<0.05, **=p<0.01; one tailed Wilcoxon paired signed ranks test. (n=10, N=2)

(c) Cerebellar-evoked striatal responses persist when the cortex is inactivated by infusion of TTX or QX314 (n=5, N=2).

(d) Single-unit (i) (n=5) or multi-unit (ii) (n=24) recording examples of excitatory responses of neurons in the dorsolateral striatum following cerebellar stimulation in a mouse in which the motor cortices were bilaterally surgically removed (N=3).

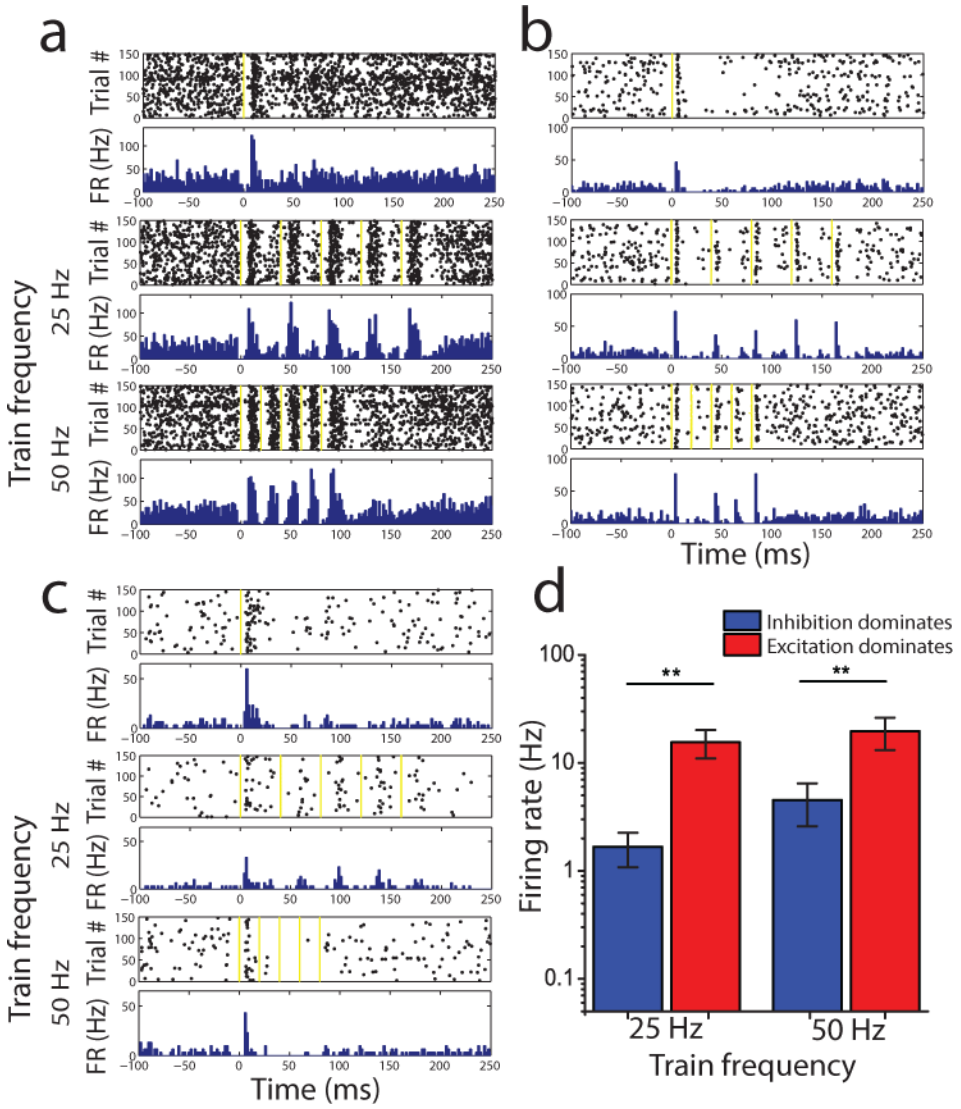

Figure 5. Striatal neurons can follow high frequency cerebellar stimulation

To examine whether the striatum can follow high frequency cerebellar activity, the dentate nucleus was electrically stimulated with 25 and 50 Hz trains. All neurons examined (n=32; N=5) could follow the high frequency trains.

(a–c) Example responses for different cells to a single pulse, 25 Hz train, and 50 Hz train at the same stimulation intensity. With high frequency stimulation excitatory responses dominated in some striatal cells and in others, inhibition. The last stimulus pulse at the end of each train was monitored to determine whether excitation persisted (examples in “a” and “b”), or inhibition dominated (50 Hz example shown in “c”).

(d) Both with 25 and 50 Hz trains, whether excitation or inhibition dominated during the train was correlated with the baseline firing rate of the striatal neuron; excitation was dominant in cells with higher baseline firing rates cells. (** = $p<0.01$; two tailed Mann-Whitney U test).

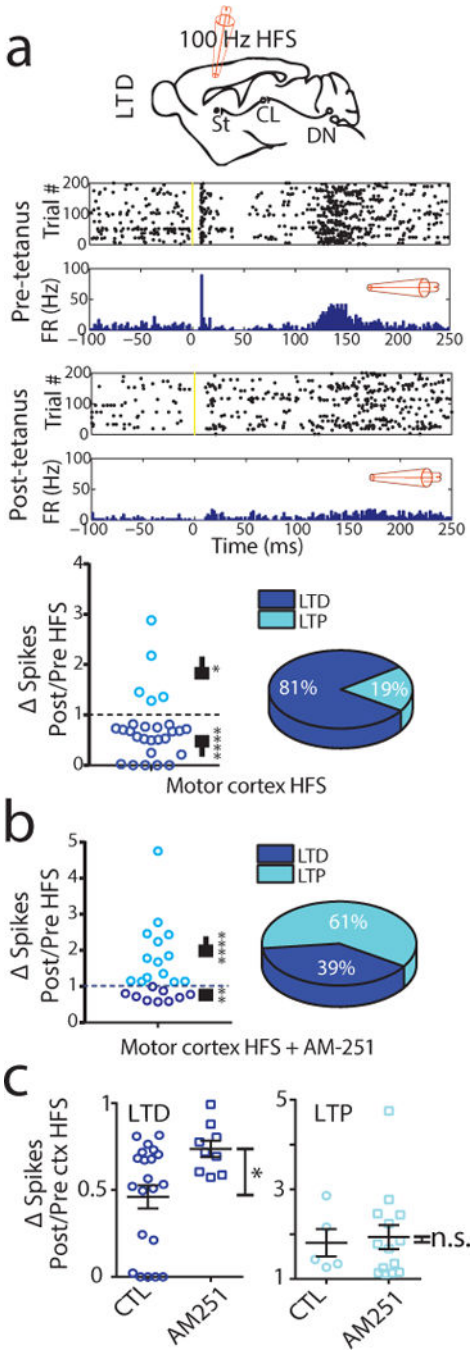

Figure 6. Corticostriatal plasticity *in vivo*

(a) Single-unit activity of dorsolateral striatal neurons was recorded in awake freely moving mice in response to activation of the motor cortex before and after high frequency stimulation of the cortex (HFS, 100 Hz). Data are presented as the ratio of the number of spikes after high frequency cortical stimulation (Δ spikes post-stimulus) to that prior to high frequency stimulation (Δ spikes pre-stimulus) with the scatter of individual cells on the left. A ratio greater than 1 indicates LTP (light blue symbols) and less than 1 indicates LTD

(dark blue symbols). (mean±S.E.M., LTD n=21, LTP n=5, N = 4, *=p<0.05, ****=p<0.0001, one-tailed, one-sample Wilcoxon signed ranks).

(b) AM-251 was injected i.p. 30 minutes before delivery of cortical HFS to test whether the plasticity induced by motor cortex HFS was cannabinoid-dependent. AM-251 injected animals showed significantly more LTP than LTD ($p < 0.0001$, Chi-squared goodness-of-fit test). The magnitude of plasticity for cells exhibiting LTD or LTP was significantly different from unity (mean±S.E.M., LTD n = 9, LTP n =14, N =3, ****=p<0.0001, **=p<0.01, one-tailed, one-sample Wilcoxon signed ranks).

(c) The magnitude of LTD was significantly less in the animals injected with AM-251 compared with those in the control animals (one tailed Mann-Whitney U test, $p < 0.05$). In contrast, the magnitude of LTP in the animals injected with AM-251 was the same as that seen in the control animals (one tailed Mann-Whitney U test, $p = 0.82$).

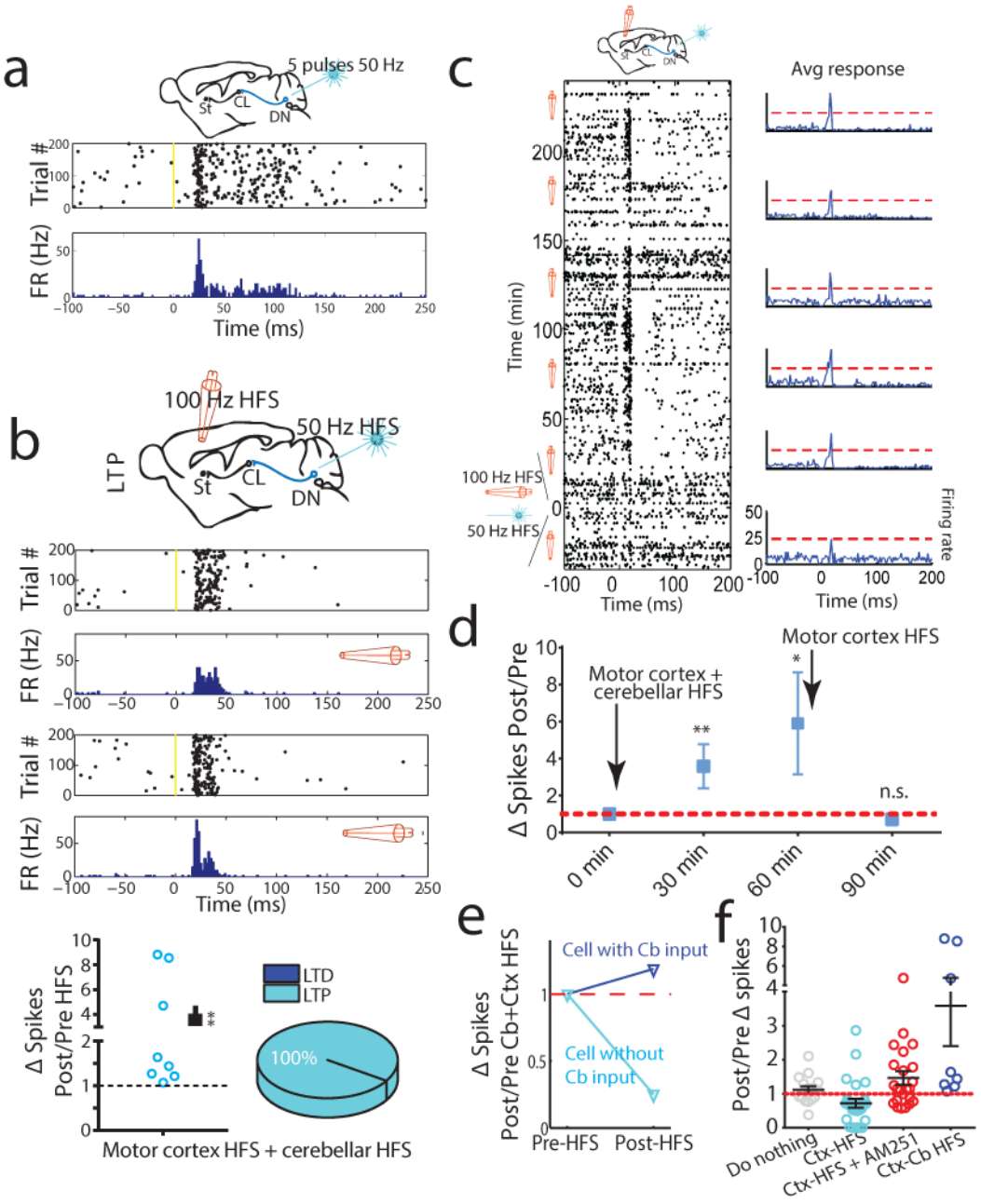

Figure 7. Cerebellar modulation of corticostriatal plasticity

(a) Cells were tested using a 5 pulse, 50 Hz train to determine whether they were reliably depolarized by cerebellar inputs.

(b) High frequency 100 Hz electrical stimulation of the cortex was combined with high frequency 50 Hz optogenetic stimulation of the dentate nucleus of the cerebellum. This HFS reliably potentiated the corticostriatal response in all the cells tested. (mean±S.E.M., LTP n=8, N=4, **=p<0.01, one-tailed, one-sample Wilcoxon signed ranks).

(c) Example cell demonstrating the timecourse of the LTP induced in (b). Time zero denotes time of paired HFS. The average firing rate of the cell as a function of time relative to HFS

is shown in the right column with the red dashed line denoting the peak firing rate of the pre-HFS response.

(d) The average change in the cortico-striatal response after concurrent HFS of the cortex and cerebellum shows clear LTP. Subsequent HFS of the cortex induced LTD in the same cells. (mean±S.E.M., *=$p<0.05$, **=$p<0.01$, one tailed Wilcoxon paired signed ranks test).

(e) Effect of simultaneous cortical and cerebellar HFS on two neighboring striatal neurons recorded with the same electrode, where one cell was responsive to cerebellar stimulation and the other was not. The cell which was excited by cerebellar stimulation underwent LTP, while the non-responsive neuron showed LTD.

(f) Comparison of the strength of plasticity induced by HFS under various experimental conditions. Also shown is the “do nothing” condition, where no HFS was delivered. ($p<0.0001$, one tailed Kruskal-Wallis test).

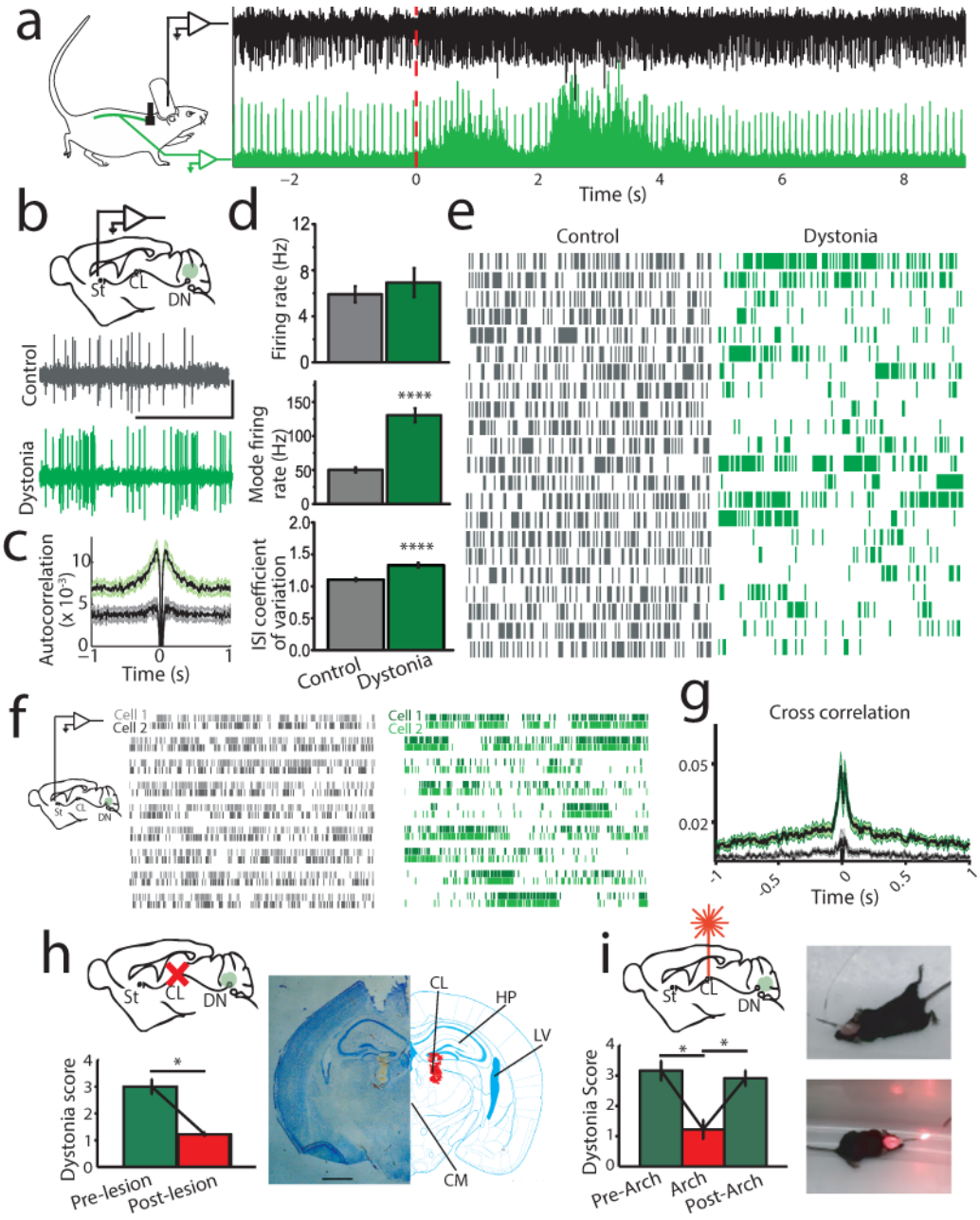

Figure 8. Cerebellar-induced dystonia is associated with dynamic interactions between the cerebellum and basal ganglia

(a) Simultaneous multi-unit (MUA) recording from dorsolateral striatum (top black trace) and field electromyography (fEMG; bottom green trace) in a mouse with cerebellar-induced dystonia. At the time indicated by the dashed red line the animal suffered a severe dystonic posture and this was reflected both as an increase in the MUA and concurrently in the fEMG record. The regular spikes throughout the fEMG correspond with the heartbeat.

(b) Single unit activity of a striatal neuron in an awake freely moving mouse recorded under normal conditions (Control, grey) and during cerebellar-induced dystonia (green). Scale bars denote 500 ms and 100 μV respectively.

(c) Average autocorrelation of striatal neuron activity before (grey) and after (green) cerebellar-induced dystonia show an increased tendency to burst firing during dystonia. The shaded areas denote S.E.M.

(d) Average firing rate, mode of the instantaneous firing rate, and the coefficient of variation (CV) of interspike intervals (ISI) in dorsolateral striatal neurons before (grey bars) and during (green bars) cerebellar-induced dystonia. While with dystonia the average firing rate of striatal neurons is not changed appreciably, their burst firing is reflected in their high predominant (mode) firing rate and in their irregular activity (indicated by the increase in ISI CV). Data are shown as mean±S.E.M. n= 139 control, 42 dystonia, ****=$p<0.0001$; two-tailed unpaired t-test.

(e) Rasters showing the spiking of representative striatal neurons recorded from control (black) and dystonic (green) mice. Each row represents 25 seconds and the same cell's activity continues from one row to the next.

(f) The Example rasters show the activity of the same two adjacent striatal neurons recorded by the same electrode before (grey) and after (green) cerebellar-induced dystonia. Each row represents 30 seconds and the cell pair's activities continue from one row to the next. During dystonia there is a significant increase in the periods of time when the two adjacent cells are active at the same time.

(g) Average cross-correlation of activity of adjacent striatal cell pairs under normal conditions (black) and during cerebellar-induced dystonia (green). The shading represents S.E.M. (n = 21 pairs).

(h) Dystonia scores in animals with cerebellar-induced dystonia before and after bilateral lesioning of the centrolateral nucleus of the thalamus (CL) are shown on the left column. The right figure shows Nissl stained section of tissue of a CL lesioned animal with matching stereotaxic atlas on right. Lesion area is marked in red. Scale bar, 1 mm. Data are presented as mean±S.E.M. HP: hippocampus, CL: centrolateral thalamic nucleus, LV: lateral Ventricle, CM: central medial thalamic nucleus. *=$p<0.05$, Wilcoxon paired signed ranks.

(i) Average dystonia scores pre, during, and post optogenetic silencing of the intralaminar thalamic nuclei in mice with cerebellar-induced dystonia. To silence neurons archaerhodpsin was expressed in the intralaminar nuclei and CL was primarily targeted by the fiber optic. The photographs show cerebellar-induced dystonia in mouse (top) and its alleviation (bottom) when laser was turned on to silence CL. *=$p<0.05$, Wilcoxon paired signed ranks.